

Supplementary Information for

Disrupting the α -synuclein-ESCRT interaction with a peptide inhibitor mitigates neurodegeneration in preclinical models of Parkinson's disease

Satra Nim[#], Darren M. O'Hara[#], Carles Corbi-Verge, Albert Perez-Riba, Kazuko Fujisawa, Minesh Kapadia, Hien Chau, Federica Albanese, Grishma Pawar, Mitchell L. De Snoo, Sophie G. Ngana, Jisun Kim, Omar M. A. El-Agnaf, Enrico Renella, Lewis E. Kay, Suneil K. Kalia[#], Lorraine V. Kalia[#], Philip M. Kim[#]

[#]These authors contributed equally

This PDF file includes:

Figures S1 to S6
Tables S1

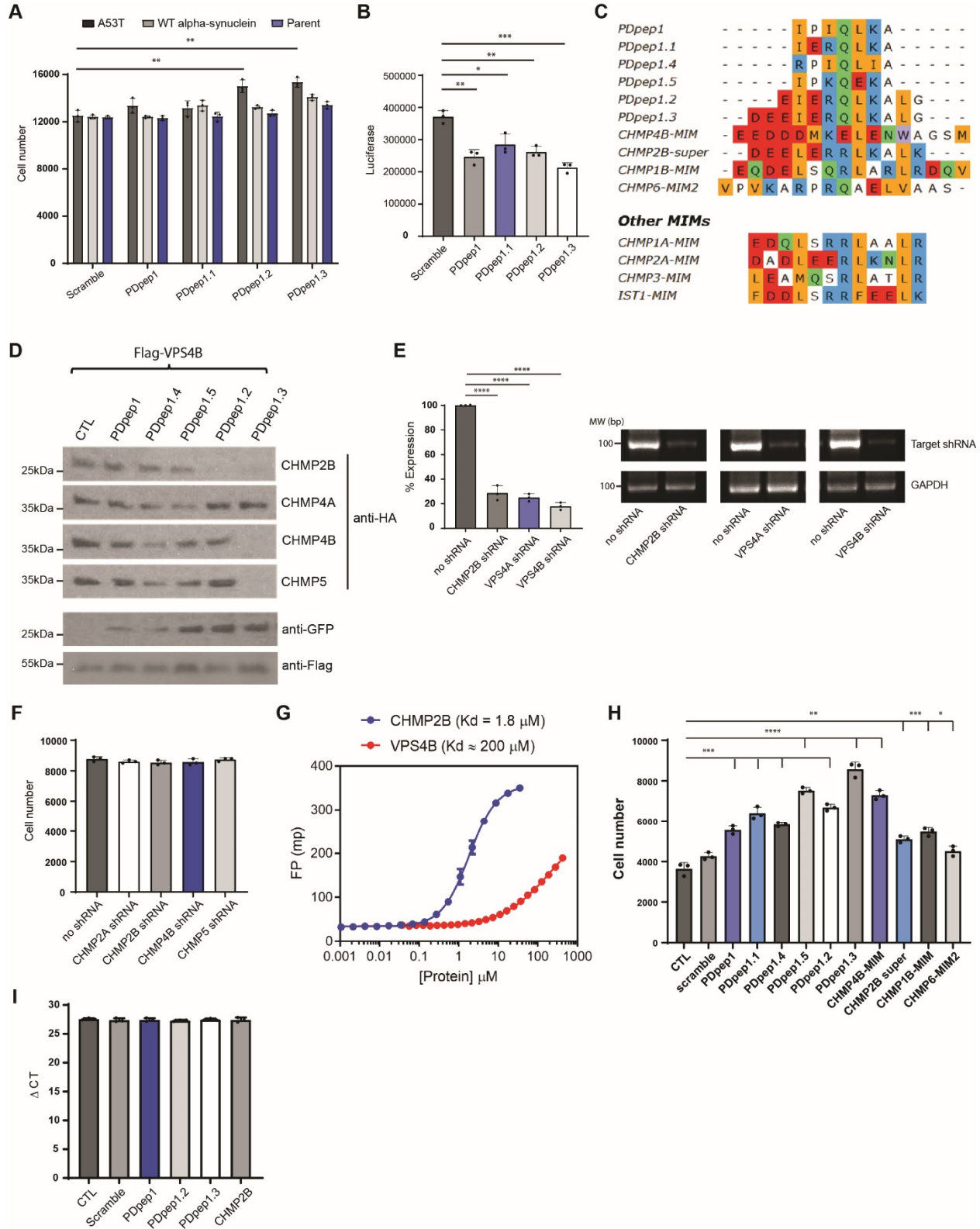


Figure S1. Additional *in vitro* validation of hits, PDpep1.3 disrupts CHMP2B-VPS4B interaction and binds more tightly to CHMP2B than VPS4B. (A) Validation of cell viability effect of peptides in A53T or (wild type (WT) a-syn expressing cells without addition of MG132. Data represent means \pm s.d. (unpaired two-tailed t-tests; PDpep1.2, $P=0.0040$; PDpep1.3, $P=0.0016$; $n=3$). (B) A53T a-syn oligomers as measured by luciferase activity. All 4 peptides showed significant reduction in A53T a-syn oligomers in cells stably expressing split luciferase a-syn constructs. Data represent means \pm s.d. (unpaired two-tailed t-tests; PDpep1, $P=0.0019$; PDpep1.1, $P=0.0166$; PDpep1.2, $P=0.0020$; PDpep1.3, $P=0.0004$; $n=3$). (C) Overlapping sequences of different MIMs as displayed in Ugene (1) and aligned with ClustalW (2). CHMP1B-MIM represents a classic MIM, and CHMP2B-super is a version of PDpep1.3 modified to be closer to a classic MIM. (D) Co-immunoprecipitation experiments to test for PPI disruption. Flag-VPS4B was immunoprecipitated in the presence of different HA-tagged CHMP proteins and GFP-tagged peptides. PDpep1.3 disrupted the interaction between VPS4B and CHMP2B. We used GFP alone as a control (CTL). (E) Reduction in gene expression level with shRNA knockdown. Expression of targeted gene was measured in cells stably expressing shRNA as indicated. Experiments were done in triplicate. Data represent means \pm s.d. (unpaired two-tailed t-tests; CHMP2B shRNA, $P<0.0001$; VPS4A shRNA, $P<0.0001$; VPS4B shRNA, $P<0.0001$; $n=3$). (F) Effects of shRNA gene knockdown in A53T a-syn expressing cells on cell viability. Data represent means \pm s.d. ($n=3$). (G) Fluorescence polarization (FP) binding assay of a FITC-labeled DEEIERQLKALG peptide against CHMP2B ($Kd=1.8 \mu\text{M}$) (blue) and VPS4B ($Kd \sim 200 \mu\text{M}$) (red). (H) Effect of MIM motif peptides (illustrated in C) on cell viability in A53T a-syn expressing cells. We used GFP alone as a control (CTL). Data represent mean values \pm s.d. (unpaired two-tailed t-tests; PDpep1, $P=0.0008$; PDpep1.1, $P=0.0004$; PDpep1.4, $P=0.0003$; PDpep1.5, $P<0.0001$; PDpep1.2, $P=0.0001$; PDpep1.3, $P<0.0001$; CHMP4B-MIM, $P<0.0001$; CHMP2B-super, $P=0.0019$; CHMP1B-MIM, $P=0.0010$; CHMP6-MIM2, $P=0.0181$; $n=3$). (I) ΔCt values for the RT-PCR data in Figure 2A showing no difference in a-syn levels. Data represent means \pm s.d. ($n=3$). * $P<0.05$; ** $P<0.01$; *** $P<0.001$; **** $P<0.0001$. Source data are provided as a Source Data file.

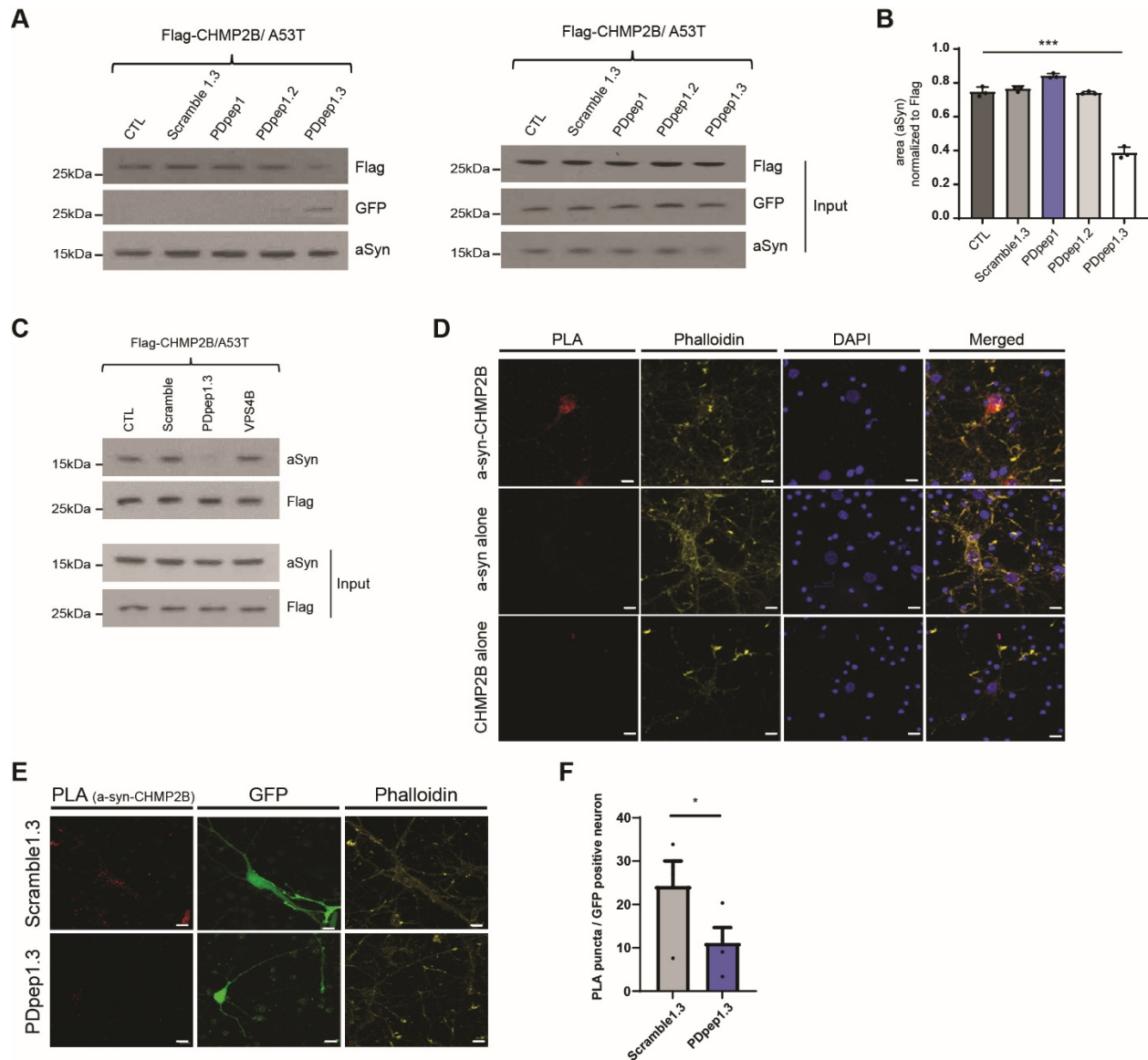


Figure S2. PDpep1.3 outcompetes a-syn binding to CHMP2B. (A) Validation of PPI disruption using reverse co-immunoprecipitation assays. HA-tagged A53T a-syn was immunoprecipitated in the presence of Flag-CHMP2B and GFP-tagged peptides. For controls, we included GFP alone (CTL) and a GFP-tagged scrambled version PDpep1.3 (Scramble1.3). (B) Quantification of immunoblot bands for a-syn (normalized to Flag from Figure 3A (left panel)). Data represent means \pm s.d. (unpaired two-tailed t-test, $t(4)=2.7764$; PDpep1.3, $P=0.0002$; $n=3$). (C) Validation of PPI disruption using co-immunoprecipitation assays. Flag-CHMP2B was immunoprecipitated in the presence of HA-tagged A53T a-syn and GFP-tagged peptides or VPS4B ($n=3$). (D) Representative confocal images of *in situ* proximity ligation assay (PLA) signal (red) indicating a physical interaction between a-syn and CHMP2B in rat primary cortical neurons (stained with phalloidin) (top panels). Negative controls for the assay include anti-a-syn antibodies alone (middle panels) or anti-CHMP2B antibodies alone (bottom panels) ($n=10$ fields of view; scale bars=5 μ m). (E) Representative confocal images of *in situ* PLA signal, indicating an a-syn-CHMP2B interaction, which is lower in rat primary cortical neurons transduced with PDpep1.3-

GFP compared with Scramble1.3-GFP (scale bars=5 μm). **(F)** Quantification of number of PLA puncta in GFP positive neurons. Bars represent means \pm s.e.m. (unpaired two-tailed t-test, $t(18)=2.881$; $P=0.0099$; $n=4$). ** $P<0.01$; *** $P<0.001$. Source data are provided as a Source Data file.

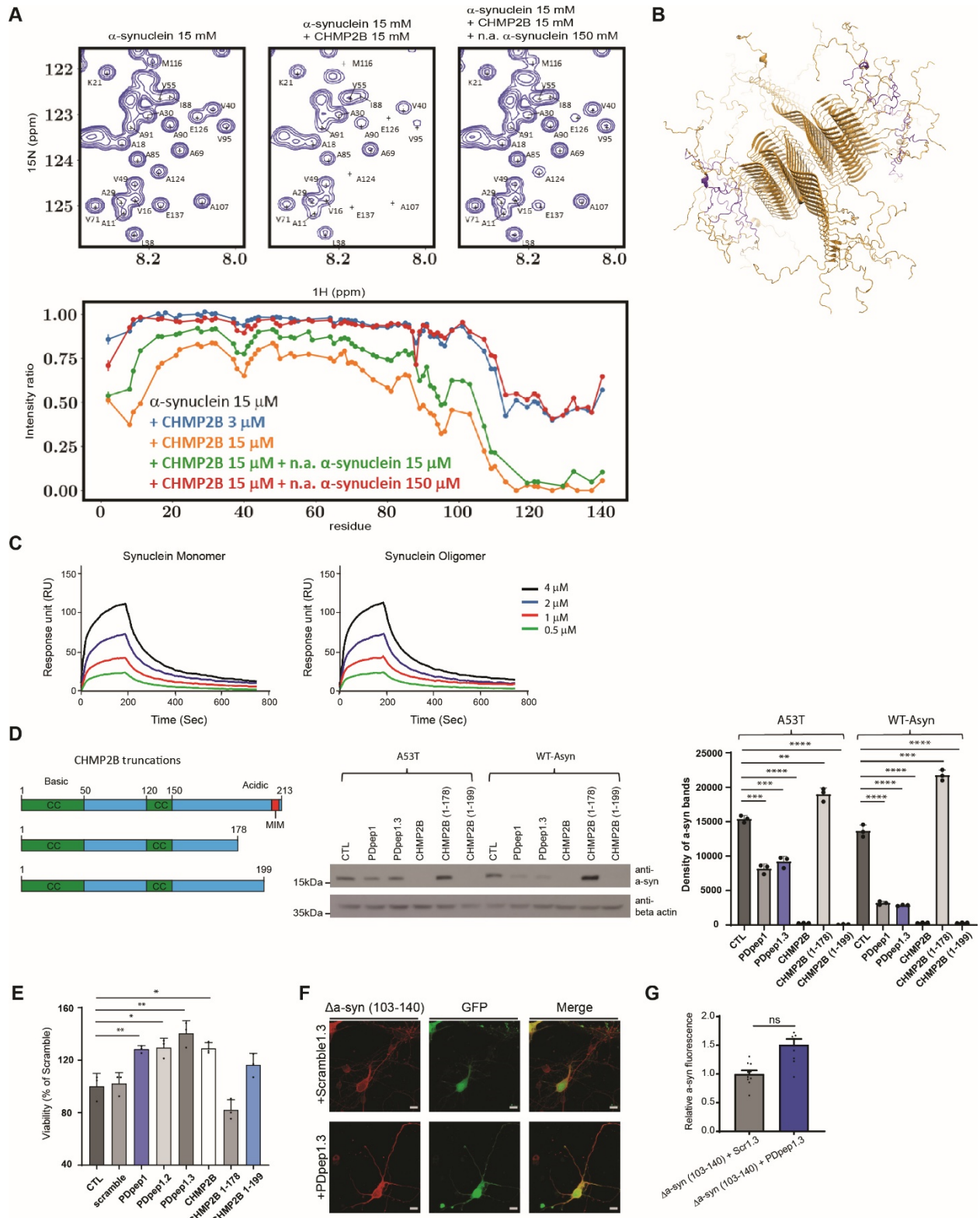


Figure S3. CHMP2B interacts with the C-terminus of a-syn. (A) Interaction between a-syn and CHMP2B probed by solution NMR spectroscopy. Top: Regions of ^{15}N , ^1H HSQC spectra for U- ^{15}N a-syn alone (left panel), in the presence of 1:1 CHMP2B (middle panel), and in the presence

of both 1:1 CHMP2B and 10-fold excess of natural abundance (n.a.) a-syn (right panel). Bottom: Ratios of intensities vs. residue number. The numerator of the ratios is indicated by the figure legend, while the denominator is the intensity of U-15N a-syn alone. The profiles for the samples in red and blue indicate that approximately 12 μ M of CHMP2B are sequestered by the presence of 150 μ M a-syn and corresponding to a K_d of \sim 20 μ M. **(B)** Structure of a-syn and binding region to CHMP2B (in violet). PDB ID is 2N0A, and the residues in violet are 103-NEEGAPQEGILE-114. **(C)** Surface plasmon resonance (SPR) binding assay of CHMP2B against a-syn monomer ($K_d=1.82$ μ M) and a-syn oligomer ($K_d=1.37$ μ M). **(D)** Schematic of CHMP2B truncations. PDpep1, PDpep1.3, and CHMP2B 1-199 truncation are each associated with a reduction in a-syn levels by immunoblot. Quantification of a-syn levels is shown in the bar graph. Data represent means \pm s.d. (unpaired two-tailed t-tests; A53T PDpep1, $P=0.0001$; A53T PDpep1.3, $P=0.0004$; A53T CHMP2B, $P<0.0001$; A53T CHMP2B (1-178), $P=0.0044$; A53T CHMP2B (1-199), $P<0.0001$; WT-Asyn PDpep1, $P<0.0001$; WT-Asyn PDpep1.3, $P=0.0001$; WT-Asyn CHMP2B, $P<0.0001$; WT-Asyn CHMP2B (1-178), $P=0.0003$; WT-Asyn CHMP2B (1-199), $P<0.0001$; $n=3$). **(E)** Cell viability assay in A53T a-syn cell line with peptides and truncated CHMP2B proteins. Data represent means \pm s.d. (unpaired two-tailed t-tests; PDpep1, $P=0.0091$; PDpep1.2, $P=0.0143$; PDpep1.3, $P=0.0073$; CHMP2B, $P=0.0101$; $n=3$). **(F)** Representative images of rat primary cortical neurons transduced with a truncated version of A53T a-syn lacking amino acids 103-140 (Δ a-syn (103-140)) which was HA-tagged plus Scramble1.3-GFP or PDpep1.3-GFP (scale bars=5 μ m). **(G)** Quantification of relative Δ a-syn(103-140) fluorescence (by immunostaining with anti-HA antibodies) in GFP positive neurons. Bars represent means \pm s.e.m. (two-tailed nested t-test, $t(57)=2.722$; $P=0.0529$; $n=3$). * $P<0.05$; ** $P<0.01$; *** $P<0.001$; **** $P<0.0001$; ns indicates $P>0.05$. Source data are provided as a Source Data file.

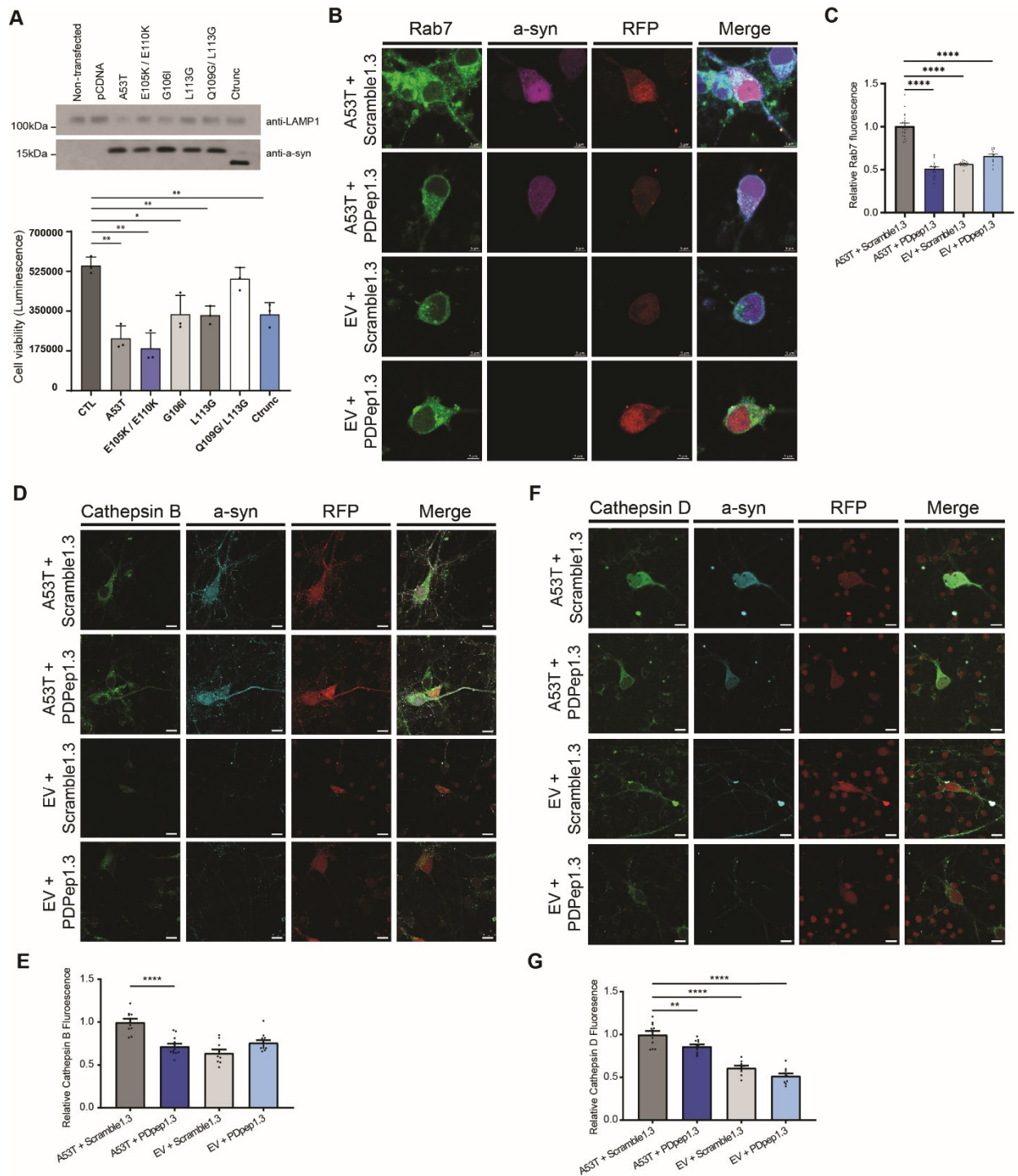


Figure S4. Endolysosomal markers are disrupted by a-syn and normalized by PDpep1.3. (A) Effects of a-syn mutations in the CHMP2B binding region on LAMP1 levels (upper panel) and cell viability (lower panel). Data represent means \pm s.d. (unpaired two-tailed t-tests; A53T, $P=0.0012$; E105K/E110K, $P=0.0013$; G106I, $P=0.0154$; L113G, $P=0.0024$; Ctrunc, $P=0.0044$; $n=3$). (B) Representative images of primary cortical neurons transduced with A53T a-syn or EV plus Scramble1.3-RFP or PDpep1.3-RFP and immunostained for Rab7 and a-syn (scale bars=5

μm). **(C)** Quantification of Rab7 fluorescence in RFP positive neurons. Bars represent means \pm s.e.m. (one-way ANOVA, $F(3, 142)=43.07$; $P<0.0001$ followed by Dunnett's post-test; $n=3$). **(D)** Representative images of rat primary cortical neurons transduced with A53T a-syn or EV plus Scramble1.3-RFP or PDpep1.3-RFP and immunostained for cathepsin B and a-syn (scale bars= $10\ \mu\text{m}$). **(E)** Quantification of cathepsin B fluorescence in RFP positive neurons. Bars represent means \pm s.e.m. (one-way ANOVA, $F(3, 40)=18.44$; $P<0.0001$ followed by Dunnett's post-test; $n=3$). **(F)** Representative images of rat primary cortical neurons transduced with mutant A53T a-syn or EV plus Scramble1.3-RFP or PDpep1.3-RFP and immunostained for cathepsin D and a-syn (scale bars= $10\ \mu\text{m}$). **(G)** Quantification of cathepsin D fluorescence in RFP positive neurons. Bars represent means \pm s.e.m. (one-way ANOVA, $F(3, 40)=57.07$; $P<0.0001$ followed by Dunnett's post-test; $n=3$). * $P<0.05$; ** $P<0.01$; **** $P<0.0001$. Source data are provided as a Source Data file.

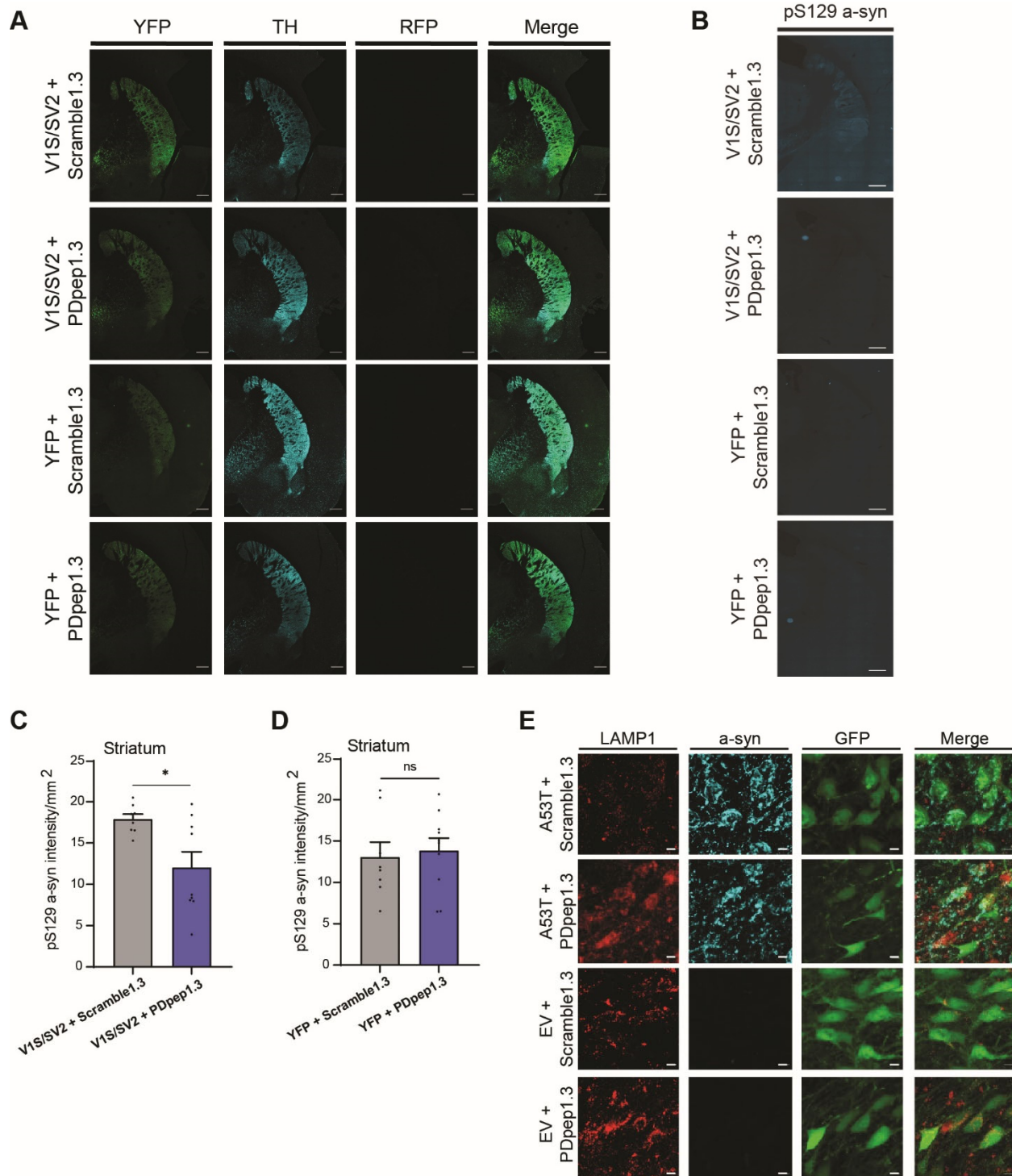


Figure S5. PDpep1.3 rescues TH and pS129 a-syn levels in striatum and increases LAMP1 levels in SN. (A) Representative images of the striatum of rats injected with V1S/SV2 or YFP plus Scramble1.3-RFP or PDpep1.3-RFP showing (A) immunostaining with anti-tyrosine hydroxylase (TH) antibody and native fluorescence (YFP or RFP) or (B) immunostaining with anti-pS129 a-syn antibody (scale bars=500 μ m). Quantification of pS129 a-syn fluorescence in rat striatum at 6 weeks post injection of (C) V1S/SV2 plus Scramble1.3-RFP or PDpep1.3-RFP (unpaired two-

tailed t-test, $t(15)=2.787$; $P=0.0138$; Scramble1.3, n=8 rats; PDpep1.3, n=9 rats) or **(D)** full length YFP plus Scramble1.3-RFP or PDpep1.3-RFP (unpaired two-tailed t-test, $t(16)=1.040$; $P=0.31$; Scramble1.3, n=8 rats; PDpep1.3, n=10 rats). Bars represent means \pm s.e.m. **(E)** Representative z-stack projection images showing immunostaining (with anti-LAMP1 or anti-a-syn antibodies) and native GFP fluorescence in substantia nigra (SN) of rats injected with low-titer A53T a-syn plus Scramble-GFP or PDpep1.3-GFP (top two panels); or low-titer EV plus Scramble-GFP or PDpep1.3-GFP (bottom two panels) (scale bars=10 μ m). * $P<0.05$; ns indicates $P>0.05$. Source data are provided as a Source Data file.

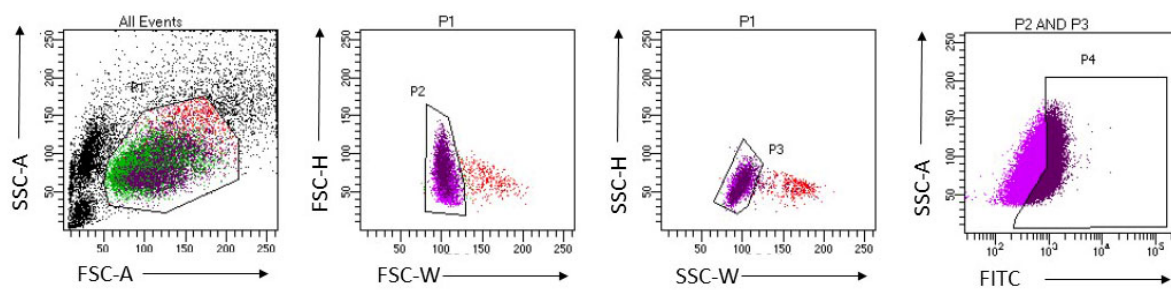


Figure S6. Flow cytometry gating. Representative flow cytometric gating hierarchy used for data shown in Figure 3F.

WT a-syn cytotoxicity screen							
Peptide	Reads 0μM MG132	Reads 10μM MG132	Reads 25μM MG132	Reads 50μM MG132	Slope Norm Reads	# Mapped Complexes	# PD GO Terms
IPIQLKA	90	1	1629	3375	3.45	11	16
RAPSCHL	1	13	33	-	0.15	2	50
DWLMVNL	1	13	29	-	0.13	3	5
LPASMPG	2	16	27	-	0.09	1	0
LQVGVAV	1	25	23	-	0.09	13	18
PLPTGMG	1	3	20	-	0.08	7	8
CMVHSAG	4	14	33	-	0.08	1	1
AAYNLCA	1	14	19	-	0.07	6	18
LSGECVP	3	28	28	-	0.07	9	27
GAAAGGT	1	10	17	-	0.06	70	162

A53T a-syn cytotoxicity screen							
Peptide	Reads 0μM MG132	Reads 10μM MG132	Reads 25μM MG132	Reads 50μM MG132	Slope Norm Reads	# Mapped Complexes	# PD GO Terms
IPIQLKA	168	20	3859	13308	40.54	11	16
QSVVTAP	8	6	37	465	1.38	16	30
CKYRSVL	5	7	11	438	1.30	4	9
PAMQIDG	32	20	53	337	0.96	6	4
GWTTVRR	15	1	29	322	0.94	0	0
QSVLQQV	13	2	12	282	0.82	8	37
QSPSSAW	9	45	59	284	0.82	19	46
QVSVAQQ	45	13	120	246	0.69	9	18
QAELSNS	6	8	10	235	0.69	5	39
EDVNKCV	6	6	13	233	0.68	4	11

A53T a-syn oligomers screen						
Peptide	Reads GFP Neg	Reads GFP Inter	Reads GFP High	Reads Ratio	# Mapped Complexes	# PD GO Terms
IPIQLKA	15556	2853	12	1,218.98	11	16
WPRYPHI	92	0	1	47.36	2	1
CFLFQIQ	88	0	1	45.32	0	0
ECHTKIR	76	0	1	39.21	2	9
MQMKLSQ	70	0	1	36.15	6	45
TQKRELT	69	0	1	35.64	7	21
VYLDILG	59	0	1	30.55	7	2
LKRDQPV	118	0	3	30.30	21	103
NNQYSFV	58	0	1	30.04	10	29
LPSKIYK	57	0	1	29.53	14	167

Table S1. Peptide counts from the screens. Illumina sequencing results after demultiplexing, demonstrating peptide counts. Only reads with an average quality Phred score of >30 were

selected, and frequencies were calculated. Reads were then normalized to the total number of peptides read for that sample population, and a scalar factor was applied.

Supplementary References:

1. K. Okonechnikov, O. Golosova, M. Fursov, Unipro UGENE: a unified bioinformatics toolkit. *Bioinformatics* **28**, 1166-1167 (2012).
2. M. A. Larkin *et al.*, Clustal W and Clustal X version 2.0. *Bioinformatics* **23**, 2947-2948 (2007).